Peer reviewed version

Link to published version (if available):
10.1021/acs.jpclett.6b02280

Link to publication record in Explore Bristol Research
PDF-document

University of Bristol - Explore Bristol Research
General rights

Observation of Electronic Excitation Transfer Through Light Harvesting Complex II Using Two-Dimensional Electronic–Vibrational Spectroscopy

Nicholas H. C. Lewis[†‡§], Natalie L. Gruenke[†‡§], Thomas A. A. Oliver[†‡§],

Matteo Ballottari[∥], Roberto Bassi[∥], and Graham R. Fleming[*†‡§]

[†] Department of Chemistry, University of California, Berkeley, California 94 720, United States

[‡] Molecular Biophysics and Integrated Bioimaging Division, Lawrence Berkeley National Laboratory, Berkeley, California 94720, USA

[§] Kavli Energy Nanoscience Institute at Berkeley, Berkeley, California 94720, USA

[∥] Dipartimento di Biotecnologie, Facoltà di Scienze, Universitá di Verona, Strada Le Grazie, I-37134 Verona, Italia

Abstract

Light-harvesting complex II (LHCII) serves a central role in light harvesting for oxygenic photosynthesis and is arguably the most important photosynthetic antenna complex. In this work, we present two-dimensional electronic–vibrational (2DEV) spectra of LHCII isolated from spinach, demonstrating the possibility of using this technique to track the transfer of electronic excitation energy between specific pigments within the complex. We assign the spectral bands via comparison with the 2DEV spectra of the isolated chromophores, chlorophyll *a* and *b*, and present evidence that excitation energy between the pigments of the complex are observed in these spectra. Finally, we analyze the essential components of the 2DEV spectra using singular value decomposition, which makes it possible to reveal the relaxation pathways within this complex.

Introduction

Light-harvesting complex II (LHCII) is the major photosynthetic antenna complex for higher plants. It comprises a substantial fraction of the protein content in the thylakoid membrane and binds a majority of the chlorophyll (Chl) *a* and *b* found in plants.(1) In the membrane, LHCII forms a trimer with pseudo-C_3 symmetry. Each monomer binds 14 Chl molecules, typically 8 Chl *a* and 6 Chl *b*, as well as four carotenoids–two luteins, one neoxanthin and one violaxanthin, which is believed to interconvert according to the violaxanthin–antheraxanthin–zeaxanthin cycle.(2) The positions of the chlorophyll molecules inside the LHCII trimer are shown in Figure 1. The Chls serve primarily as light-harvesting pigments, absorbing solar photons and transferring the electronic excitation energy to the photosystem II (PSII) reaction center. The role of the various carotenoids is rather more complex, as they can function both in light harvesting and in photoprotection.(3-9)

LHCII is responsible for the majority of light absorption associated with PSII. Because of this central role in oxygenic photosynthesis, the structure and the detail of the electronic excitation dynamics in LHCII have been thoroughly characterized,(2) using a wide variety of techniques, ranging from X-ray crystallography,(10, 13) genetic manipulation,(14, 15) and structure-based modeling(12, 16) to a broad variety of steady-state and time-resolved spectroscopies,(17-24) including a series of recent studies utilizing two-dimensional electronic spectroscopy (2DES).(25-28) However, there remain limits on our understanding that are imposed, in large part, by the limitations of the techniques that have been hitherto available.

All spectroscopic methods which rely solely on interaction with electronic transitions suffer from the same defect, which is related ultimately to the difficulty in separating the effects of differences in electronic site energies of individual pigments and of electronic coupling between pigments. Electronic transitions occur between eigenstates of the electronic Hamiltonian, which in complex systems are often not easily related to the site basis of actual pigments and their positions. This fact necessitates sophisticated modeling efforts to provide the link between the electronic spectroscopies and the actual flow of the excitation energy through the complex, which is typically the goal of these studies. A variety of techniques based on a combination of structural and spectroscopic information have been developed to address this issue for photosynthetic light-harvesting complexes,(16, 29) and progress has also been made in addressing these questions using quantum chemistry techniques,(30-34) but a significant degree of ambiguity and uncertainty remains. Additional complexities arise from

the fact that the site basis is generally the natural basis in which to describe the environment and the interactions between the environment and the electronic excited states, and that the strength of the coupling to the environment is typically of the same order of magnitude as the strength of the electronic coupling between pigments, and the thermal energy $k_{\mathrm{B}}T$. Thus, accurate quantum dynamics simulations must rely on computationally expensive exact methods(35, 36) or on approximation schemes that must balance accuracy with cost.(12, 16, 37, 38) The spatial organization of the electronic eigenstates according to the best currently available Hamiltonians developed using these modeling procedures is shown in Figure 1, but an experimental approach capable of directly providing this link between the electronic eigenstates and the site basis would be of great value in the research of photosynthetic light harvesting.

Recently, we have proposed an experimental method by which this direct link might be obtained, based on 2D electronic–vibrational (2DEV) spectroscopy.(39, 40) 2DEV spectroscopy is a two-color coherent multidimensional spectroscopic technique that is capable of directly correlating the electronic transitions of a molecule with its vibrational structure, by using a combination of visible and mid-infrared (IR) laser pulses.(39, 41, 42) The essential idea is to leverage the local character of certain high frequency Chl vibrational modes, and use these localized vibrations as a proxy for position within the large protein complex. The pigments are located in different positions within the protein, and are therefore exposed to slightly different electrostatic fields induced by the protein. Furthermore, the differences in the various binding pockets induce different minor structural deformations in the Chls located at each binding site and bind the Chl to the protein using different axial ligands and hydrogen bonding configurations.(10) Together, these effects cause shifts in the frequencies of various high energy vibrations, making it possible, in principle, to identify specific sites by their vibrational bands. These are the same effects which result in different electronic energies for each site. However, unlike the electronic absorption spectrum, which is determined by both the site energies as well as the electronic couplings, the vibrational spectrum of the individual pigments is not likely to be strongly affected by dipole interactions with neighboring pigments. Therefore, as long as it is possible to assign vibrational bands to specific pigments, it should be possible to use 2DEV spectroscopy to directly relate the electronic excitation spectrum and the excited state energy transfer dynamics to specific sites within the complex.

Here, we present 2DEV spectra of the Chl *a* and Chl *b* Q bands in isolated LHCII trimers and demonstrate how different bands display different dynamics, depending on both the electronic state that is excited as well as the vibration that is probed. Some of these features, such as the relaxation from Chl *b* sites to Chl *a* sites, are easy to assign, and provide us with an unambiguous measurement of these relaxation dynamics, potentially revealing discrepancies with the best available Hamiltonians for LHCII. Other vibrational bands are more difficult to localize and at present can only be tentatively assigned based on their dynamics and the available Hamiltonians. These results compare favorably to previous transient IR spectra of LHCII, which—because of the nature of transient absorption spectroscopy—suffered from limitations in spectral and temporal resolution, hindering the degree of information that could be extracted.(43) We expect that a combination of mutant studies, theoretical calculations of vibrational electrochromic shifts, and high level QM/MM simulations will make the assignments of these bands possible, thereby placing these measurements among the most detailed experimental studies of the electronic relaxation dynamics in LHCII, or any other photosynthetic light-harvesting complex, to date.

We present the discussion of the results in three parts. First we provide assignments for the major features observed in the 2DEV spectra of LHCII, given in comparison to 2DEV spectra of isolated Chl *a* and Chl *b*. Then we qualitatively describe the dynamics observed in the spectra. Finally, we perform a principle component analysis of the LHCII spectra based on the singular value decomposition (SVD) and provide a more quantitative analysis of the time scales and dynamics observed in these spectra.

2DEV spectra of isolated Chl *a* and Chl *b* and of LHCII at an early waiting time $t_2 = 0.25$ ps, prior to the majority of the exciton transfer and relaxation, are shown in Figure 2. The features in spectra of the isolated chromophores have been assigned in detail in previous work,(44) but for clarity we will briefly discuss them here. These spectra are dominated by several broad structures along the detection axis ω_3. The intense bleach features at $\omega_3 = 1655$ cm^{-1} in the Chl *a* spectra and at 1665 cm^{-1} in the Chl *b* spectra are assigned to C=O stretch modes, while the broad excited state absorptions peaking near 1610 cm^{-1} are most likely due to the analogous modes on the electronic excited states. Less intense bleaches are observed at 1550 cm^{-1} and, as depletions in the excited state feature near 1590 cm^{-1}, are assigned to chlorin ring-stretching modes. Along the excitation axis ω_1 of the Chl *a* spectra, two major features are observed, at 14 650 and 15 400 cm^{-1}, corresponding to excitation of the electronic transitions that dominate

the visible linear absorption spectrum–the lower energy Q_y band, and the higher energy band that arises from a vibronic mixture of Q_y and Q_x.(45) In the Chl b spectra shown in Figure 2b, the Q_y band dominates at $\omega_1 = 15\,000$ cm^{-1}, and the Q_x associated bands appear as weak features near $\omega_1 = 16\,500$ cm^{-1}. In addition to these major spectral features, there are also weaker bands which are important to discuss, particularly a weak bleach band in the Chl a spectra at $\omega_1 = 14\,900$ cm^{-1} and $\omega_3 = 1680$ cm^{-1} and two moderate intensity bands in the Chl b spectra at $\omega_1 = 15\,350$ cm^{-1}, a bleach at $\omega_3 = 1690$ cm^{-1}, and an excited state absorption at 1640 cm^{-1}. These features are due to the five-coordinate Chl molecules, where the central Mg is axially bound to only a single solvent molecule, as opposed to the major features of the spectra, which arise from the six-coordinate species, axially coordinated by two solvent molecules.(44) According to the crystal structure of LHCII,(10) the majority of the Chl pigments are either four- or five-coordinate, and so the spectral positions of these peaks should be expected to be more similar to the features observed in the LHCII spectra.

The 2DEV spectrum of LHCII shown in Figure 2c shows several bands that can be readily related to the spectra of Chl a and Chl b. The spectrum shows two major electronic excitation bands at $\omega_1 = 14\,800$ and $15\,400$ cm^{-1}, as well as a low intensity shoulder to higher excitation energies. These structures can be understood in direct relationship to the LHCII linear visible absorption spectrum shown in Figure 1b. The $14\,800$ cm^{-1} band has been assigned as a combination of several electronic states associated with Chl a Q_y transitions, whereas the $15\,400$ cm^{-1} band arises primarily from Chl b transitions, with some contribution from higher energy Chl a states.(12, 25) Presumably, this band also contains contributions from Chl a Q_x transitions, which in isolation occur at a similar energy. The higher energy shoulder, which extends past $16\,500$ cm^{-1}, is due to the Q_x transitions and higher energy vibronic excitations. Along the detection axis ω_3, there are several features which can be directly assigned based on comparison to the 2DEV spectra of the isolated chromophores. Slices through the Chl a, Chl b and LHCII spectra at $\omega_1 = 14\,800$ and $15\,400$ cm^{-1} are shown in Figure 2d,e to facilitate the comparison between these spectra. The bleach feature at $\omega_1 = 15\,400$ cm^{-1} and $\omega_3 = 1690$ cm^{-1} is a clear indication of populated Chl b in LHCII, being located at precisely the same spectral location as the bleach of the five-coordinate Chl b in the isolated chromophore. The two prominent positive features in the LHCII spectrum located at $\omega_1 = 14\,800$ cm^{-1} and at $\omega_3 = 1660$ and 1680 cm^{-1} undergo identical dynamics and most likely arise from the same underlying band, corresponding to the ground electronic state C=O stretch of the Chl a, with an interfering excited state band at $\omega_3 = 1670$ cm^{-1}. An excited state band corresponding to the

same vibrational mode can be clearly observed at the early waiting times for initial excitation to the higher energy electronic band, at $\omega_1 = 15\,400$ cm^{-1}. It is unclear whether this excited state band corresponds to a mode on Chl a, on Chl b or on both, as this band does not appear in the 2DEV spectra of the isolated chromophores. Another possibility is that this band arises from distortions induced in nearby protein vibrations due to the excitation of a Chl. According the 2.72 Å crystal structure, a number of the Chl ligands are coordinated to the side chain of a glutamate moiety (a602, b609, a610), an asparagine moiety (a612) or a glutamine moiety (a613), or to a backbone carbonyl (b601, b605). Each of these amino acids possess vibrational modes with frequencies near 1670 cm^{-1},[46] mostly with C=O stretch character. If the frequency or absorption strength of these protein modes is altered by the electronic excitation of the coordinated Chl, this could potentially explain the appearance of the new induced absorption band.

In addition to these bleach bands, which can be used to identify excited state population on Chl a and Chl b, the bleach of a chlorin ring stretching mode is observed at $\omega_3 = 1555$ cm^{-1} across the whole excitation band. This band appears to be blue-shifted by ~5 cm^{-1} relative to the corresponding band in the spectra of the isolated pigments. This shift can be explained by interactions between the pigments and the protein. The Chls bound to proteins are generally not entirely planar, as observed in the crystal structure,[10] due to the coordination state and the structures of the binding pockets. Furthermore, many of the pigments are in close proximity to charged amino acid residues, so the shift of this band could also be caused by some combination of the vibrational electrochromic shift induced by the electrostatic charges of the protein,[47-49] and hydrogen bonding interactions.

The 2DEV spectra of LHCII shown in Figures 2c and 3a–d are dominated by broad negative features, which correspond to absorption by vibrations on the electronic excited states. In addition to the narrow feature at 1670 cm^{-1} we have already described, these absorption features are composed of two major bands, centered at $\omega_3 \simeq 1590$ and 1640 cm^{-1} and arise from excitation anywhere in the visible absorption spectrum. The gap between these absorption features at $\omega_3 = 1620$ cm^{-1} is caused by interference with a bleach feature that can be observed in the transient infrared absorption spectrum and appears in the $t_2 < 0$ ps vibrational perturbed free induction decay. The intense, broad absorption feature is most likely related to the Chl C=O stretch modes on the electronic excited states. The ~100 cm^{-1} width of this band is caused

by the effect of the different protein environments experienced by each chlorophyll in the complex. It appears that the protein induced frequency shifts significantly broaden the electronic excited state features relative to the ground state bands. This is likely due to the greater polarizability and more diffuse character of electronic excited states, which would likely magnify the vibrational shifts due to nearby electrostatic interactions. The dynamics of different portions of this band, then, should provide specific information about the electronic populations of the different Chl moieties in the LHCII and make it possible to track the flow of electronic excitation energy through the complex.(40)

The evolution of the LHCII 2DEV spectrum with respect to the waiting time t_2 is illustrated in Figure 3a–d. The time points that are easiest to understand are the early time spectrum shown in Figure 3a, before most electronic energy transfer occurs, and the long time spectrum shown in Figure 3d, at $t_2 = 15$ ps. The latter, which is subsequent to the majority of the transient excitation transfer dynamics, shows a significant degree of symmetry between the two major electronic excitation bands. The structures in the spectra can be most readily interpreted in relation to theoretical simulations of the 2DEV spectra of an electronically coupled dimer.(40) The $t_2 = 0$ ps spectrum is representative of the distribution of excited state population initially created by the visible excitation laser. For each excitation frequency ω_1, the spectrum with respect to the detection frequency ω_3 is given by the vibrational spectrum of the sites which can be populated by a visible excitation at ω_1. The weight in the spectrum of each individual site is provided by the participation of that site in the exciton states excited by that excitation energy. The loss of strong dependence on ω_1 at longer waiting times t_2 indicates that the excitation energy in the complex has largely approached its equilibrium distribution with respect to the excited state manifold. It is believed to take ~50 ps for excitation energy in LHCII to fully equilibrate.(12) The dependence of the spectral intensity on ω_1 depends primarily on the amount of population initially created with that energy; therefore, this aspect of the structure is not expected to relax.(40) For LHCII at 77 K, when the electronic excited states have equilibrated, the majority of the population will be localized on the low energy trimer composed of the sites a610, a611, and a612.(12) This $t_2 = 15$ ps spectrum, then, should be described reasonably well as the 2DEV spectrum of these three sites, with the ratio of each given by their relative population at equilibrium, independent of the excitation energy.

Between the limiting cases of the initial excitation distribution observed in the $t_2 = 0$ ps spectrum and the long time spectrum of the roughly equilibrium populations, 2DEV spectra at intermediate times contain the details of excited state energy transfer and relaxation. To facilitate the visualization of the effect of the excitation energy transfer between the various chromophores in the complex, we plot slices through the two main electronic excitation bands at $\omega_1 = 14\,800$ and $15\,400$ cm^{-1} in Figure 3e,f. Here, the dynamics have been normalized to the fit to the first right singular vector $V_1(t)$, which represents the overall relaxation of the spectrum, and will be discussed in greater detail subsequently.

The dynamics that are easiest to interpret are those of the bleach features related to Chl b at $\omega_1 = 15\,400$ cm^{-1} and $\omega_3 = 1690$ cm^{-1}, which decays with increasing t_2. At the same time, the bleach associated with Chl a at $\omega_1 = 15\,400$ cm^{-1} and $\omega_3 = 1680$ and 1660 cm^{-1} grows in. These are clear, unambiguous indications of excited state population that was initially created in Chl b undergoing energy transfer to Chl a. The Chl a bleach features located at $\omega_1 = 14\,800$ and $15\,400$ cm^{-1} can be compared to separately track the population that originated on Chl b and other high energy excited states from that which originated on the lower energy Chl a states. Notably, there is a shoulder at $\omega_3 = 1690$ cm^{-1} for all excitation frequencies that persists out to long time. This feature may be an indication of a long-lived excited state population on Chl b, even when the lower energy electronic absorption band traditionally assigned as Chl a has been excited. According to the Novoderezhkin Hamiltonian for LHCII,[12] the lowest energy electronic eigenstate which contains at least 10% of its population on a Chl b lies 310 cm^{-1} above the overall lowest energy exciton. Although this might be sufficient to explain the presence of this shoulder at $\omega_1 = 14\,800$ cm^{-1} for early waiting times, it cannot explain its persistence with t_2: the thermal energy at 77 K is insufficient to populate this state subsequent to exciton relaxation. This observation of long-lived Chl b population, therefore, suggests that there may be a significant problem with the currently available Hamiltonians for LHCII and that there are low energy states with significant Chl b character. Even if these observations are further substantiated, it seems unlikely that the overall connectivity of the current Hamiltonians is incorrect, as this is determined in large part by the crystal structure for LHCII. The models used to estimate the site energies and coupling strengths, however, will certainly have to be reevaluated.

In addition to the dynamics of these bleach features specifically associated with either Chl a or Chl b, the broad excited state absorption feature also of significant interest. They can be roughly

separated into three regions which display different kinetics: two narrower bands at $\omega_3 \simeq 1650$ and 1635 cm^{-1}, and a broad region encompassing ~1560–1620 cm^{-1} (centered near 1590 cm^{-1}). The dynamics of these bands are somewhat different for the slices corresponding to excitation at ω_1 = 14 800 or 15 400 cm^{-1}, but they share some similar features. For both excitation regions the 1650 cm^{-1} band shows an overall decay, on the time scale of several picoseconds (ps). This is in sharp contrast with the neighboring band at 1635 cm^{-1}, which shows an initial increase in intensity on a sub-ps time scale. For the lower energy excitation at ω_1 = 14 800 cm^{-1}, this band then levels off and remains roughly constant for the remainder of the waiting time. For the higher energy excitation at ω_1 = 15 400 cm^{-1}, however, following a similar initial rise, this vibrational band subsequently decays, after several ps. The 1590 band behaves differently, showing a monotonic increase in intensity for both excitation regions. Following an initial sub-ps time scale shared between the two excitation bands, for the higher energy excitation this increase slows substantially, and the intensity remains roughly constant, whereas it continues to gain intensity for the lower energy excitation region.

Together, the dynamics of these modes suggest a flow of excitation energy through the complex. Under this interpretation, the ω_3 = 1650 cm^{-1} band serves as a proxy for the population of some higher energy electronic excited states, which are most likely associated with Chl *b* moieties, corresponding in frequency to the band in the Chl *b* spectrum at ω_3 = 1640 cm^{-1} and have previously assigned as most likely being due to the formyl group that differentiates Chl *b* from Chl *a*. The significant initial population of the band even for lower excitation energies typically associated with Chl *a* states, together with the fast relaxation corroborates the suggestion in the bleach bands of a greater degree of mixing between some Chl *a* and Chl *b* states than has typically been proposed. As the excitation relaxes from these higher energy states, it flows through some transient intermediates, which contribute to the 1660 cm^{-1} band, and end up in the low energy states, manifesting in the broad 1590 cm^{-1} band. Because the dynamics are somewhat different for the higher and lower energy electronic bands, there must of course be a number of chromophores that contribute to each of these vibrational bands, and so the differing dynamics show that there are distinct energy transfer pathways from the regions of the protein in which lower energy Chl *a* states are located, separate from those regions containing the higher energy, predominantly Chl *b* states. Because of the similarities in the dynamics, however, there must also be common pathways through which a substantial amount of the excitation energy is transported.

The spectral structures and dynamics illustrated in Figure 3 are quite complex. To perform a more quantitative analysis of these electronic excited states dynamics, the utilization of data reduction techniques, such as the singular value decomposition (SVD), becomes essential.(50, 51) In performing this decomposition, we consider the total spectrum $S(\omega_1, t_2, \omega_3)$ as a mapping between a vector space composed of 2D spectral surfaces $U_i(\omega_1, \omega_3)$ and their associated dynamics $V_i(t_2)$ and linearly weighted by the singular values Σ_i, so that the spectrum can be written as a matrix product $\mathbf{S} = \mathbf{U} \cdot \mathbf{\Sigma} \cdot \mathbf{V}^\dagger$. This decomposition provides a set of basis spectra that, taken together with the singular values Σ_i, describe the overall 2DEV spectrum. The most straightforward way to understand the SVD components is that the first component is the single spectrum and dynamics that best describe the total data. If this component is subtracted off, then the second component is the best spectrum and dynamics to describe the remainder, and so forth. Upon performing the SVD, we find that there are four components that are not dominated by noise. These components are shown in Figure 4, with the left singular vectors U_i (the spectral component) shown in panels (a–d) and the corresponding right singular vectors V_i (the dynamics component) shown in panel (e). To describe the kinetics of the right singular vectors, we have performed fits to biexponential decays of the form $V_i(t_2) = A_1 \exp(-t_2/\tau_1) + A_2 \exp(-t_2/\tau_2) + A_3$ for the data from $t_2 = 0$ ps onward. The results of these fits, together with the singular values for the significant components, are provided in Table 1.

The first spectral component U_1 shows very similar structures to the spectrum at $t_2 = 1$ ps, as seen in Figure 3b. This is indicative of the fact that the overall changes to the spectrum with respect to t_2 are relatively minor, with the major features remaining essentially unchanged. The dynamics in the first right singular vector V_1 reflect the overall decay of the spectrum as the excited state population returns to the ground state. The kinetics are described by two components with similar amplitudes, time constants of $\tau_1 = 1.13$ ps and $\tau_2 = 9.97$ ps, with the slower nanosecond scale relaxation captured by the constant offset.

The other three significant components can be most easily understood as describing the evolution of the spectrum with respect to the overall relaxation captured by $U_1(\omega_1, \omega_3)$ and $V_1(t_2)$. The spectral components U_2, U_3, and U_4 are rather complicated, but there are several features for which we have made the assignments, which aids in the interpretation of the associated dynamics. U_2 is the only SVD component other than U_1 that shows a significant peak at the position of the Chl b ground state C=O stretch at $\omega_1 = 15\,400$ cm^{-1} and $\omega_3 = 1690$ cm^{-1}, as well as at the prominent Chl b excited state band at $\omega_3 = 1640$. This indicates that a

significant process represented by this component is the relaxation from Chl b to Chl a. The dynamics in V_2 show a very fast 50 fs fit component, commensurate with the time resolution of the experiment, and a 0.5 ps fit component. The latter time scale is consistent with the typical time scale reported for the Chl b to Chl a energy transfer, which was first measured by fluorescence upconversion to occur with a time constant of 0.68 ps,[17] and has been measured more recently using transient absorption and 2DES to occur with two time scales of ~100–200 fs and $\lesssim 1$ ps.[12, 25, 28] The current experiment, however, has an advantage over these previous measurements, as it does not require any assumption that the excitation at the 15 400 cm^{-1} band populates only Chl b states or that there is no strong mixing between the Chl a and Chl b states; we can monitor vibrational bands that we know uniquely and unambiguously distinguishes population of Chl b and Chl a.

In addition to the readily assignable features associated with Chl b, the second, third and fourth SVD components show dynamics in the excited state absorption bands which can be related to our earlier qualitative discussion of the dynamics. U_2, which is associated with a very fast, sub-ps decay, has a negative feature at $\omega_1 = 15\,400$ cm^{-1} and $\omega_3 = 1650$ cm^{-1}, as well as a positive feature at $\omega_3 = 1640$ cm^{-1}. Together, these suggest a simultaneous decay of one excited state band, and rise of a separate band, showing the energy transfer between one set of Chls and another. The differences in the spectral structures for excitation at $\omega_1 = 15\,400$ cm^{-1} versus at $\omega_1 = 14\,800$ cm^{-1} demonstrate that the relevant dynamics, despite occurring on the same time scale, are following different pathways. In particular, for the higher energy excitations U_2 has a significant positive feature at $\omega_3 = 1640$ cm^{-1} that is absent for the lower energy excitations. This represents a gain in this part of the excited state band following the same dynamics as the decay of these Chl b states, indicating a Chl a intermediate that is quickly populated by the relaxation of these higher energy states which is bypassed by the Chl b excited at lower energies, which relax directly to the band at $\omega_3 = 1620$ cm^{-1}. With precise assignments, this should make it possible to identify which Chl a and b moieties are involved in unexpectedly large mixing, but by following the Novoderezhkin Hamiltonian, we can conclude that overall these fast dynamics are likely a signature of either the stromal side relaxation from the b601′–b608–b609 cluster to the a602–a603 cluster and the a610–a611–a612 low energy trimer, or of the lumenal side relaxation from the b606–b607 dimer to the a604–b605 dimer. The third SVD component shows a rise component with a time scale of 0.46 and 4.21 ps and is associated with a negative spectral feature at $\omega_3 = 1600$ cm^{-1}, which seems then to describe the long time rise

of the excited state band in this region of the spectrum. Presumably, this band should be related to the low energy trimer a610–a611–a612 which contribute to the lowest energy electronic states, and perhaps the bottleneck sites a604, a613–a614, and a602–a603. The fourth SVD component shows a fast 0.45 ps rise followed by a 4.21 ps decay and is associated with a negative band at $\omega_3 = 1645$ cm^{-1}. This feature must be related to some short-lived intermediates, such as b605, which might act as an important intermediate in the Chl b to Chl a energy transfer. This seems reasonable, as it is also associated with a positive band near the Chl b 1690 cm^{-1} ground state feature, but has its intensity peaked instead at $\omega_3 = 1685$ cm^{-1} and therefore may be a shifted Chl b bleach band. The Novoderezhkin Hamiltonian[12] predicts the popluation on b605 to decay to a604 on a 3.6 ps time scale, which is in good agreement with our observed kinetics. The details of these spectral components suggest that if it is possible to accurately assign the specific vibrational shifts of each Chl molecule in the LHCII complex, these data will reveal specific energy transfer pathways that would be very difficult to resolve with conventional time-resolved electronic spectroscopies.

In this work, we have presented and discussed the structures and dynamics observed in 2DEV spectra of the photosynthetic light-harvesting complex LHCII. The major features of the spectrum are assigned by comparison to the 2DEV spectra of isolated Chl a and Chl b. However, there are some significant differences, the details of which are difficult to precisely assign. The substantial advantage of this method over traditional electronic spectroscopic techniques comes from the unambiguity with which it can be possible for molecular vibrational bands to be assigned to specific molecular species, as opposed to the broad, relatively structureless electronic transitions. The major difficulty for this system is in making the assignments in a large and complex system. An analysis of the vibrational shift induced by the protein due to effects such as specific conformational distortions, hydrogen bonding, coordination state, and shifts induced by the electrostatic fields of the protein environment will provide greater insight into the detailed assignments of the observed vibrational bands. Advances in quantum chemistry methods that would allow for the exploration of excited state potential surfaces of large and complex systems like LHCII would be of great value toward complete understanding of the photophysics of photosynthetic light harvesting.

We use the dynamics of the spectrum, coupled with a SVD spectral analysis, to demonstrate how 2DEV can be used to follow the flow of excitation energy through the complex. The distinct vibrational bands of the Chl a and Chl b allow us to directly track the energy transfer

between these different species, with no ambiguities due to imprecise electronic Hamiltonians or broad electronic line widths. For the vibrational bands that we can definitively assign to a specific molecular species, we can track the motion of the electronic excitation energy through the complex without relying on modeling and spectral fitting. For example, the spectral decomposition reveals signatures of a short-lived (~5 ps) Chl b intermediate, which is most likely associated with the b605 site. The long-lived shoulder at $\omega_3 = 1690$ cm^{-1} band and amplitude in the excited state band at $\omega_3 = 1650$ cm^{-1} provide evidence that we observe a completely unexpected Chl b population that survives for longer than 25 ps, which is not predicted by the currently available Hamiltonians. If this interpretation is correct, this would bring into question the quality of these models and would suggest that the details of the exciton transfer dynamics through LHCII need to be substantially reconsidered.

The 2DEV experiments furthermore allow us to observe dynamics in the electronic excited state bands that provide more detailed information about the flow of excitation energy through the complex. We observe distinct bands which report on the different phases of the early relaxation of the excitation energy through the complex. Current computational techniques make it very difficult to provide these excited state vibrational bands with definitive assignments due in large part to the importance of the environmentally induced shifts, and the cost of excited state quantum chemistry methods. If it becomes possible to determine precise assignments of the vibrational band on the electronic excited state for the different sites in the complex, then these experiments will provide us with unparalleled resolution of the early time flow of electronic excitation energy through the LHCII complex.

Experimental Methods

The details of the 2DEV technique have been detailed previously.(39) The experiment was driven with a Ti:Saph oscillator and regenerative amplifier (Micra, Legend Elite, Coherent), which was used to pump a home-built visible NOPA and a home-built mid-IR OPA. The visible pump covered the region ~14 250–16 700 cm^{-1}, to span the Q bands of the Chl a and Chl b absorption spectra. The infrared laser was centered at 1620 cm^{-1}, resonant with the high frequency Chl carbonyl and chlorin ring C=C stretching vibrational modes. The first time delay t_1 between the visible pump pair was generated and controlled using a pulse shaper (Dazzler, Fastlite), and the experiments were performed in the partially collinear "pump-probe" geometry. t_1 was scanned from 0–75 fs in 1.5 fs steps for the LHCII data and in 2.5 fs steps for

the Chl a and b data in the fully rotating frame. Each visible pulse was compressed using the pulse shaper together with a SF14 prism pair to ~15 fs, as characterized by self-referenced spectral interferometry(52) (Wizzler, Fastlite). The total excitation power was attenuated to ~325 nJ and focused with a f = 25 cm silver-coated 90° off-axis parabolic mirror to a spot size of ~250 μm.

To measure the changes in the infrared absorption along the detection axis ω_3, the infrared probe laser was dispersed on a spectrometer, imaged onto a dual-array 64 element HgCdTe detector (Infrared Systems Development). To mitigate the effect of shot-to-shot laser noise in the IR, the signal was normalized against a reference beam. At the sample, each IR laser beam has a total pulse energy of ~100 nJ and a duration of ~60 fs. The beams were focused at the sample using a f = 15 cm gold-coated 90° off-axis parabolic mirror to a spot size of ~200 μm. The entire IR laser setup was purged with dry, CO_2-free air provided by a lab gas generator (Parker Balston).

The waiting time t_2 between the visible pump pair and the IR probe was controlled with a motorized delay stage. The relative polarization of the pump and probe lasers was set to either parallel (giving rise to the signal $S_\parallel$) or perpendicular ($S_\perp$), and the isotropic responses were calculated as $S_{\text{iso}} = S_\parallel + 2\,S_\perp$. The desired 2DEV signal was isolated by phase cycling the pump pulse pair in a 4 × 1 scheme,(53, 54) and a Fourier transform was performed along t_1 to produce the final electronic excitation frequency ω_1 vs vibrational detection frequency ω_3 correlation spectra, parametrized by the waiting time t_2.

The LHCII sample was isolated from spinach, and dispersed in a buffer of 50 mM Tris–HCl (pH 7.8), 0.12 M NaCl, 0.3 M sucrose, and 0.03% n-dodecyl β-D-maltoside in D_2O. This solution was mixed with glycerol-d_8 in a 70:30 (v/v) glycerol:LHCII ratio. The sample cell was constructed from two CaF_2 plates with a kapton spacer, and had a path-length of 100 μm and was placed in an optical cryostat (OptistatDN2, Oxford Instruments) at 77 K. The maximum optical density in the visible, shown in Figure 1, was 0.8 and was ~0.4 in the solvent subtracted infrared absorption (dominated by the protein amide bands). The Chl *a* and Chl *b* samples were dissolved in ethanol-d_6, held at 77 K in the same type of sample cell. These samples had optical

density of 2 at the absorption maximum in the visible, and of ~0.1 in the solvent-subtracted infrared absorption.

Author Present Address

(T.A.A.O.) School of Chemistry, University of Bristol, Bristol BS8 1TS, United Kingdom.
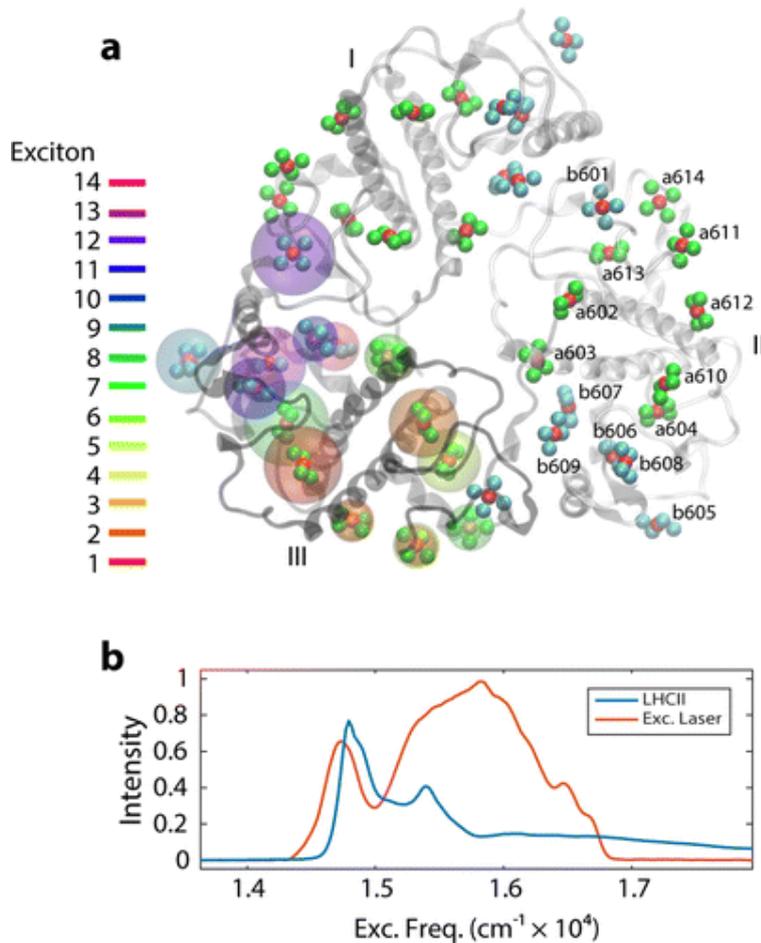
Figure 1

Figure 1. (a) Structure of LHCII trimer viewed from the stromal surface, from the 2.72 Å X-ray crystal structure.(10, 11) The Chl *a* and *b* are represented by their Mg (red spheres) and N (Chl *a* green, Chl *b* cyan). The carotenoids and lipids are omitted for clarity. The Chl ligands in monomer II are labeled with the crystal structure numbers. The Chl ligands in monomer III are marked with colored orbs, where the color indicates the 14 exciton states. The size of each orb indicates the degree to which that site contributes to the exciton, according to the Novoderezhkin Hamiltonian.(12) (b) Electronic absorption spectrum of LHCII at 77 K, together with the normalized excitation laser spectrum.
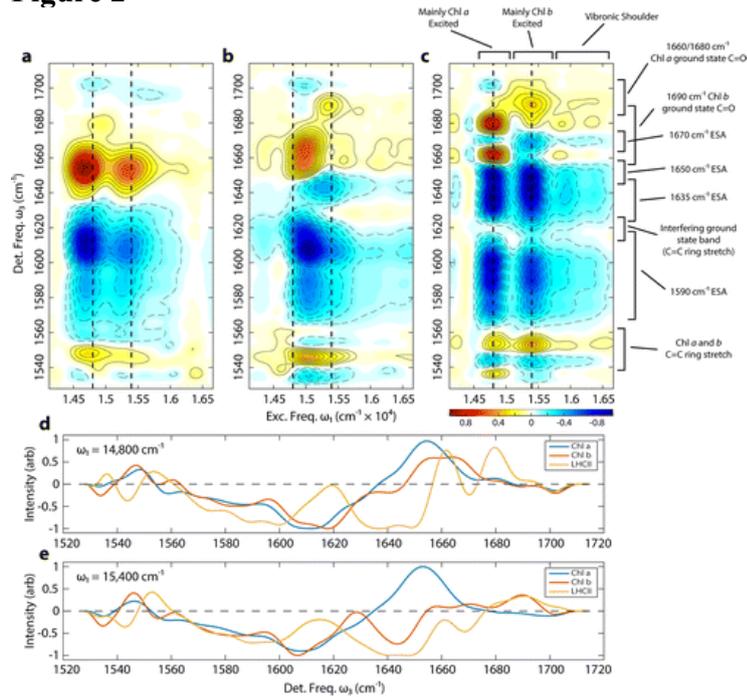
Figure 2

Figure 2. 2DEV spectra of Chl *a* (a), Chl *b* (b), and LHCII (c) at $t_2 = 250$ fs. The positive features shown in yellow-red and solid contours indicate the bleach of the vibrational modes on the ground excited state, and the negative features shown in blue and dashed contours indicate absorptions by vibrations on the electronic excited states. Each spectrum is normalized relative to its own absolute maximum. The dashed lines at $\omega_1 = 14\,800$ and $15\,400$ cm^{-1} mark the location of the slices shown in (d) and (e). The assignments of the bands of the LHCII spectrum (c) have been labeled.
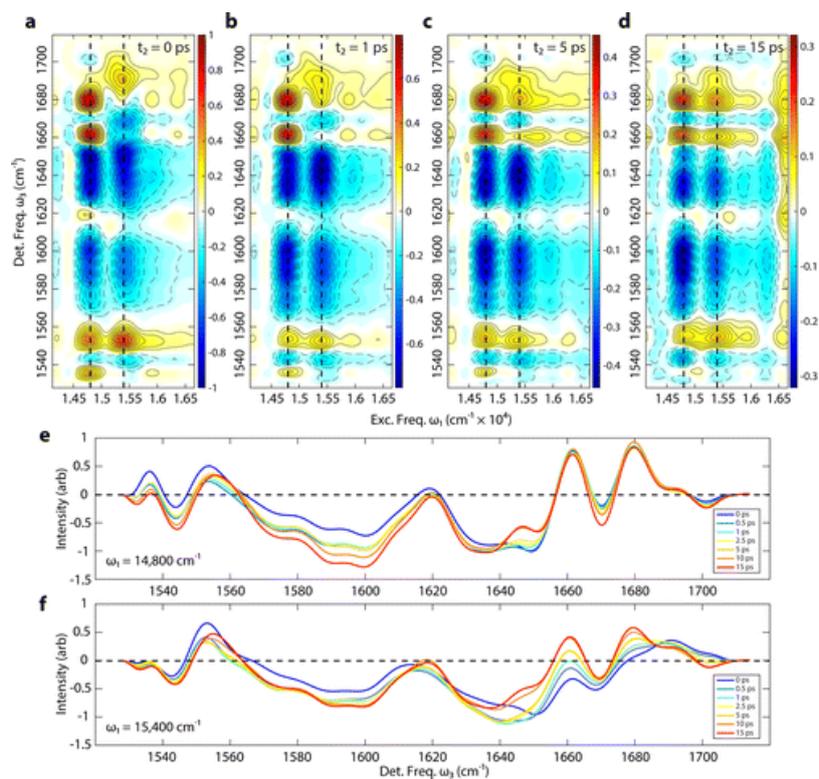
Figure 3

Figure 3. 2DEV spectra of LHCII at $t_2 = 0$ ps (a), 1 ps (b), 5 ps (c), and 15 ps (d). Slices through these spectra at $\omega_1 = 14\,800$ and $15\,400$ cm^{-1}, the positions marked by vertical dashed lines on (a–d), are shown in (e) and (f) normalized to their absolute maxima at $t_2 = 0$, where the dynamics have been normalized by the fit to the first right singular vector V_1 to facilitate visualization of the excited state dynamics, with the overall relaxation removed.
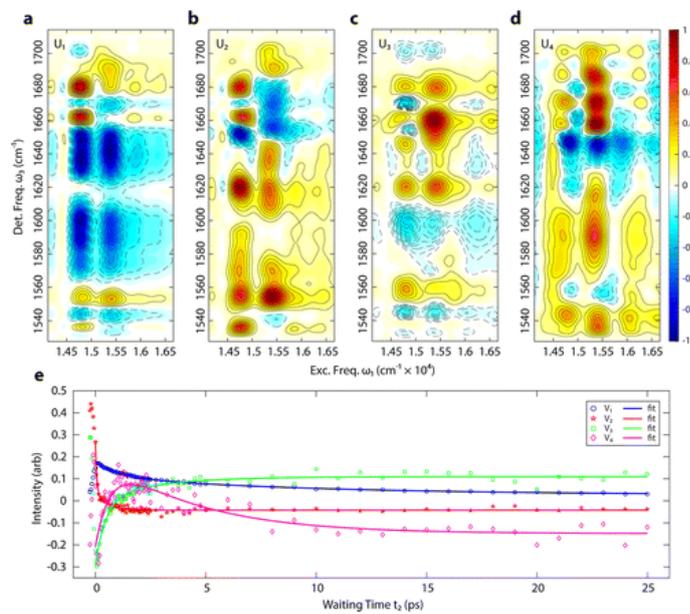
Figure 4

Figure 4. Singular value decomposition of the LHCII 2DEV spectrum. The first four left singular vectors (spectral component) are shown in (a–d), normalized to their individual absolute maxima. The corresponding right singular vectors (dynamics component) are shown in (e), with fits to biexponential decays from $t_2 = 0$ onward. The fit parameters are given in Table 1.

Table 1

Table 1. Fits to the Significant Right Singular Vectors Following the Biexponential Form $A_1\exp(-t/\tau_1) + A_2\exp(-t/\tau_2) + A_3$

	$V_i(t) = A_1\exp(-t/\tau_1) + A_2\exp(-t/\tau_2) + A_3$				
singular value Σ_i	A_1	τ_1 (ps)	A_2	τ_2 (ps)	A_3
29.25	0.07	1.13	0.08	9.97	0.03
4.46	0.22	0.05	0.09	0.50	−0.04
2.92	−0.30	0.46	−0.10	2.90	0.11
1.42	−0.45	0.67	0.39	4.21	−0.15

References

1. Blankenship, R. E. Molecular Mechanisms of Photosynthesis; Blackwell Publishing: Hoboken, NJ, 2002.

2. van Amerongen, H.; Croce, R.; van Amerongen, H.; Croce, R. Primary Processes of Photosynthesis, Part 1; Royal Society of Chemistry: Cambridge, U.K., 2007; pp 329–367.

3. Frank, H. A.; Cogdell, R. J. Carotenoids in Photosynthesis Photochem. Photobiol. 1996, 63, 257–264.

4. Walla, P. J.; Yom, J.; Krueger, B. P.; Fleming, G. R. Two-Photon Excitation Spectrum of Light-Harvesting Complex II and Fluorescence Upconversion after One- and Two-Photon Excitation of the Carotenoids J. Phys. Chem. B 2000, 104, 4799–4806.

5. Holt, N. E.; Zigmantas, D.; Valkunas, L.; Li, X.-P.; Niyogi, K. K.; Fleming, G. R. Carotenoid cation formation and the regulation of photosynthetic light harvesting Science 2005, 307, 433–436.

6. Ruban, A. V.; Berera, R.; Ilioaia, C.; van Stokkum, I. H. M.; Kennis, J. T. M.; Pascal, A. A.; van Amerongen, H.; Robert, B.; Horton, P.; van Grondelle, R. Identification of a mechanism of photoprotective energy dissipation in higher plants Nature 2007, 450, 575–578.

7. Ahn, T.-K.; Avenson, T. J.; Ballottari, M.; Cheng, Y.-C.; Niyogi, K. K.; Bassi, R.; Fleming, G. R. Architecture of a charge-transfer state regulating light harvesting in a plant antenna protein Science 2008, 320, 794–797.

8. Liao, P. N.; Holleboom, C. P.; Wilk, L.; Kühlbrandt, W.; Walla, P. J. Correlation of Car S1→Chl with Chl→Car S1 energy transfer supports the excitonic model in quenched light harvesting complex II J. Phys. Chem. B 2010, 114, 15650–15655.

9. Fuciman, M.; Enriquez, M. M.; Polivka, T.; Dall'Osto, L.; Bassi, R.; Frank, H. A.The Role of Xanthophylls in Light-Harvesting in Green Plants: A Spectroscopic Investigation of Mutant LHCII and Lhcb Pigment-Proteins Complexes J. Phys. Chem. B 2012, 116, 3834– 49.

10. Liu, Z.; Yan, H.; Wang, K.; Kuang, T.; Zhang, J.; Gui, L.; An, X.; Chang, W.Crystal structure of spinach major light-harvesting complex at 2.72 A resolution Nature 2004, 428, 287– 292.

11. Humphrey, W.; Dalke, A.; Schulten, K. VMD - Visual Molecular Dynamics J. Mol. Graphics 1996, 14, 33– 38.

12. Novoderezhkin, V. I.; Marin, A.; van Grondelle, R. Intra- and inter-monomeric transfers in the light harvesting LHCII complex: the Redfield-Förster picture Phys. Chem. Chem. Phys. 2011, 13, 17093.

13. Kühlbrandt, W.; Wang, D. N.; Fujiyoshi, Y. Atomic model of plant light-harvesting complex by electron crystallography Nature 1994, 367, 614– 621.

14. Remelli, R.; Varotto, C.; Sandona, D.; Croce, R.; Bassi, R. Chlorophyll Binding to Monomeric Light-harvesting Complex: A mutation analysis of chromophore-binding residues J. Biol. Chem. 1999, 274, 33510–33521.

15. Croce, R.; Weiss, S.; Bassi, R.Carotenoid-binding Sites of the Major Light-harvesting Complex II of Higher Plants J. Biol. Chem. 1999, 274, 29613– 29623.

16. van Grondelle, R.; Novoderezhkin, V. I. Energy transfer in photosynthesis: experimental insights and quantitative models Phys. Chem. Chem. Phys. 2006, 8, 793– 807.

17. Eads, D. D.; Castner, E. W.; Alberte, R. S.; Mets, L.; Fleming, G. R. Direct observation of energy transfer in a photosynthetic membrane: chlorophyll b to chlorophyll a transfer in LHC J. Phys. Chem. 1989, 93, 8271–8275.

18. Hemelrijk, P. W.; Kwa, S. L. S.; van Grondelle, R.; Dekker, J. P. Spectroscopic properties of LHC-II, the main light-harvesting chlorophyll a/b protein complex from chloroplast membranes Biochim. Biophys. Acta, Bioenerg. 1992, 1098, 159–166.

19. Du, M.; Xie, X.; Mets, L.; Fleming, G. R. Direct Observation of Ultrafast Energy-Transfer Processes in Light Harvesting Complex II J. Phys. Chem. 1994, 98, 4736–4741.

20. Bittner, T.; Irrgang, K. D.; Renger, G.; Wasielewski, M. R. Ultrafast Excitation-Energy Transfer and Exciton-Exciton Annihilation Processes in Isolated Light-Harvesting Complexes of Photosystem-II (Lhc-II) from Spinach J. Phys. Chem. 1994, 98, 11821–11826.

21. Agarwal, R.; Krueger, B. P.; Scholes, G. D.; Yang, M.; Yom, J.; Mets, L.; Fleming, G. R. Ultrafast Energy Transfer in LHC-II Revealed by Three-Pulse Photon Echo Peak Shift Measurements J. Phys. Chem. B 2000, 104, 2908–2918.

22. Tietz, C.; Jelezko, F.; Gerken, U.; Schuler, S.; Schubert, A.; Rogl, H.; Wrachtrup, J. Single molecule spectroscopy on the light-harvesting complex II of higher plants Biophys. J. 2001, 81, 556–562.

23. Pieper, J.; Rätsep, M.; Irrgang, K. D.; Freiberg, A. Chromophore-chromophore and chromophore-protein interactions in monomeric light-harvesting complex II of green plants studied by spectral hole burning and fluorescence line narrowing J. Phys. Chem. B 2009, 113, 10870–10880.

24. Schlau-Cohen, G. S.; Yang, H.-Y.; Krüger, T. P. J.; Xu, P.; Gwizdala, M.; van Grondelle, R.; Croce, R.; Moerner, W. E. Single-Molecule Identification of Quenched and Unquenched States of LHCII J. Phys. Chem. Lett. 2015, 6, 860–867.

25. Schlau-Cohen, G. S.; Calhoun, T. R.; Ginsberg, N. S.; Read, E. L.; Ballottari, M.; Bassi, R.; van Grondelle, R.; Fleming, G. R. Pathways of Energy Flow in LHCII from Two-Dimensional Electronic Spectroscopy J. Phys. Chem. B 2009, 113, 15352–15363.

26. Calhoun, T. R.; Ginsberg, N. S.; Schlau-Cohen, G. S.; Cheng, Y.-C.; Ballottari, M.; Bassi, R.; Fleming, G. R.Quantum Coherence Enabled Determination of the Energy Landscape in Light-Harvesting Complex II J. Phys. Chem. B 2009, 113, 16291–16295.

27. Schlau-Cohen, G. S.; Calhoun, T. R.; Ginsberg, N. S.; Ballottari, M.; Bassi, R.; Fleming, G. R. Spectroscopic Elucidation of Uncoupled Transition Energies in the Major Photosynthetic Light-Harvesting Complex, LHCII Proc. Natl. Acad. Sci. U. S. A. 2010, 107, 13276–13281.

28. Duan, H.-G.; Stevens, A. L.; Nalbach, P.; Thorwart, M.; Prokhorenko, V. I.; Miller, R. J. D.Two-Dimensional Electronic Spectroscopy of Light-Harvesting Complex II at Ambient Temperature: A Joint Experimental and Theoretical Study J. Phys. Chem. B 2015, 119, 12017–12027.

29. Adolphs, J.; Renger, T.How proteins trigger excitation energy transfer in the FMO complex of green sulfur bacteria Biophys. J. 2006, 91, 2778–97.

30. Shim, S.; Rebentrost, P.; Valleau, S.; Aspuru-Guzik, A.Atomistic Study of the Long-Lived Quantum Coherences in the Fenna-Matthews-Olson Complex Biophys. J. 2012, 102, 649–660.

31. Higashi, M.; Kosugi, T.; Hayashi, S.; Saito, S.Theoretical study on excited states of bacteriochlorophyll a in solutions with density functional assessment J. Phys. Chem. B 2014, 118, 10906–10918.

32. Sisto, A.; Glowacki, D. R.; Martínez, T. J. Ab Initio Nonadiabatic Dynamics of Multichromophore Complexes: A Scalable Graphical-Processing-Unit-Accelerated Exciton Framework Acc. Chem. Res. 2014, 47, 2857–2866.

33. Chandrasekaran, S.; Aghtar, M.; Valleau, S.; Aspuru-Guzik, A.; Kleinekathöfer, U.Influence of Force Fields and Quantum Chemistry Approach on Spectral Densities of BChl a in Solution and in FMO Proteins J. Phys. Chem. B 2015, 119, 9995–10004.

34. Curutchet, C.; Mennucci, B. Quantum Chemical Studies of Light Harvesting. Chem. Rev. 2016, DOI: 10.1021/acs.chemrev.5b00700

35. Ishizaki, A.; Fleming, G. R. Unified treatment of quantum coherent and incoherent hopping dynamics in electronic energy transfer: Reduced hierarchy equation approach J. Chem. Phys. 2009, 130, 234111.

36. Ishizaki, A.; Fleming, G. R.Theoretical examination of quantum coherence in a photosynthetic system at physiological temperature Proc. Natl. Acad. Sci. U. S. A. 2009, 106, 17255–17260.

37. Ritschel, G.; Roden, J.; Strunz, W. T.; Eisfeld, A.An efficient method to calculate excitation energy transfer in light-harvesting systems: Application to the Fenna-Matthews-Olson complex New J. Phys. 2011, 13, 113034.

38. Bennett, D. I. G.; Amarnath, K.; Fleming, G. R.A Structure-Based Model of Energy Transfer Reveals the Principles of Light Harvesting in Photosystem II Supercomplexes J. Am. Chem. Soc. 2013, 135, 9164–9173.

39. Oliver, T. A. A.; Lewis, N. H. C.; Fleming, G. R. Correlating the Motion of Electrons and Nuclei with Two-Dimensional Electronic–Vibrational Spectroscopy Proc. Natl. Acad. Sci. U. S. A. 2014, 111, 10061– 10066.

40. Lewis, N. H. C.; Dong, H.; Oliver, T. A. A.; Fleming, G. R. A Method for the Direct Measurement of Electronic Site Populations in a Molecular Aggregate using Two-Dimensional Electronic-Vibrational Spectroscopy J. Chem. Phys. 2015, 143, 124203.

41. Dong, H.; Lewis, N. H. C.; Oliver, T. A. A.; Fleming, G. R. Determining the Static Electronic and Vibrational Energy Correlations via Two-Dimensional Electronic-Vibrational Spectroscopy J. Chem. Phys. 2015, 142, 174201.

42. Lewis, N. H. C.; Dong, H.; Oliver, T. A. A.; Fleming, G. R. Measuring Correlated Electronic and Vibrational Spectral Dynamics using Line Shapes in Two-Dimensional Electronic-Vibrational Spectroscopy J. Chem. Phys. 2015, 142, 174202.

43. Stahl, A. D.; Di Donato, M.; van Stokkum, I.; van Grondelle, R.; Groot, M. L. A Femtosecond Visible/Visible and Visible/Mid-Infrared Transient Absorption Study of the Light Harvesting Complex II Biophys. J. 2009, 97, 3215–3223.

44. Lewis, N. H. C.; Fleming, G. R. Two-Dimensional Electronic-Vibrational Spectroscopy of Chlorophyll a and b J. Phys. Chem. Lett. 2016, 7, 831–837.

45. Reimers, J. R.; Cai, Z.-L.; Kobayashi, R.; Rätsep, M.; Freiberg, A.; Krausz, E.Assignment of the Q-Bands of the Chlorophylls: Coherence Loss via Qx-Qy Mixing Sci. Rep. 2013, 3, 2761.

46. Barth, A. The infrared absorption of amino acid side chains Prog. Biophys. Mol. Biol. 2000, 74, 141–173.

47. Park, E. S.; Andrews, S. S.; Hu, R. B.; Boxer, S. G. Vibrational Stark Spectroscopy in Proteins: A Probe and Calibration for Electrostatic Fields J. Phys. Chem. B 1999, 103, 9813– 9817.

48. Cho, M. Vibrational solvatochromism and electrochromism: Coarse-grained models and their relationships J. Chem. Phys. 2009, 130, 094505.

49. Choi, J. H.; Cho, M. Vibrational solvatochromism and electrochromism of infrared probe molecules containing C≡O, C≡N, C═O, or C—F vibrational chromophore J. Chem. Phys. 2011, 134, 154513.

50. Shrager, R. I.; Hendler, R. W. Titration of individual components in a mixture with resolution of difference spectra, pKs, and redox transitions Anal. Chem. 1982, 54, 1147–1152.

51. Hendler, R. W.; Shrager, R. I. Deconvolutions based on singular value decomposition and the pseudoinverse: a guide for beginners J. Biochem. Biophys. Methods 1994, 28, 1–33.

52. Oksenhendler, T.; Coudreau, S.; Forget, N.; Crozatier, V.; Grabielle, S.; Herzog, R.; Gobert, O.; Kaplan, D.Self-referenced spectral interferometry Appl. Phys. B: Lasers Opt. 2010, 99, 7–12.

53. Myers, J. A.; Lewis, K. L.; Tekavec, P. F.; Ogilvie, J. P. Two-Color Two-Dimensional Fourier Transform Electronic Spectroscopy with a Pulse-Shaper Opt. Express 2008, 16, 17420.

54. Zhang, Z.; Wells, K. L.; Hyland, E. W. J.; Tan, H.-S. Phase-Cycling Schemes for Pump–Probe Beam Geometry Two-Dimensional Electronic Spectroscopy Chem. Phys. Lett. 2012, 550, 156– 161.